Chapter 16

Single-Molecule Localization Microscopy of Subcellular Protein Distribution in Neurons

Jelmer Willems, Manon Westra, and Harold D. MacGillavry

Abstract

Over the past years several forms of superresolution fluorescence microscopy have been developed that offer the possibility to study cellular structures and protein distribution at a resolution well below the diffraction limit of conventional fluorescence microscopy (<200 nm). A particularly powerful superresolution technique is single-molecule localization microscopy (SMLM). SMLM enables the quantitative investigation of subcellular protein distribution at a spatial resolution up to tenfold higher than conventional imaging, even in live cells. Not surprisingly, SMLM has therefore been used in many applications in biology, including neuroscience. This chapter provides a step-by-step SMLM protocol to visualize the nanoscale organization of endogenous proteins in dissociated neurons but can be extended to image other adherent cultured cells. We outline a number of methods to visualize endogenous proteins in neurons for live-cell and fixed application, including immunolabeling, the use of intrabodies for live-cell SMLM, and endogenous tagging using CRISPR/Cas9.

Key words Superresolution microscopy, Single-molecule localization microscopy, Stochastic optical reconstruction microscopy, Photoactivated localization microscopy, Neuron, Synapse

1 Introduction

Fluorescence microscopy is instrumental for the investigation of subcellular protein organization which is critical to understand cellular function in health and disease. The development of super-resolution microscopy techniques such as single-molecule localization microscopy (SMLM) has tremendously increased the ability to resolve protein distribution achieving resolution below 30 nm. SMLM relies on the sequential acquisition of sparse, single emitting fluorophores that label a structure of interest. The spatial isolation of individual fluorescent events allows the accurate localization of the center point of each emission event with nanometer precision. Together, the spatial coordinates of individual localizations

Jelmer Willems and Manon Westra contributed equally.

Bryan Heit (ed.), *Fluorescent Microscopy*, Methods in Molecular Biology, vol. 2440, https://doi.org/10.1007/978-1-0716-2051-9_16,

accumulated over thousands of frames are used to reconstruct a superresolved image [1] (Fig. 1a). Importantly, in SMLM the resolution of the image is no longer determined by the diffraction limit but relies on the localization precision of fluorophores and the density of localized molecules that label the structure of interest. The localization precision (σ) is determined by a number of factors such as background noise and pixel size [2], but is mostly dependent on the number of photons (N) emitted by the fluorophore as:

$$\sigma = \frac{1}{\sqrt{N}}$$

The localization density equally contributes to the resolving power: too few localizations will result in a poor reconstruction of the structure of interest. This can be formalized based on the Nyquist-Shannon sampling criterium such that to achieve a certain resolution, fluorophores have to be sampled at a density at least twice as high as the desired spatial frequency [3]. It is therefore important to optimize labeling strategies to achieve a high labeling density.

In the recent years, a multitude of SMLM approaches have been developed, including techniques such as photoactivated localization microscopy (PALM) [4, 5], (direct) stochastic optical reconstruction microscopy (d)STORM) [6, 7], point accumulation for imaging in nanoscale topography (PAINT) [8] and MINFLUX [9]. Here, we will describe the use of PALM and (d)STORM (Fig. 1b). In PALM, a low-power activation laser is used to stochastically photoactivate or photoconvert subsets of fluorescent proteins in the active state. The most commonly used fluorescent protein is mEos3.2, which switches from green to red fluorescence upon illumination by 405 nm light and yields relatively high photon counts [10]. In (d)STORM reversible blinking of organic dyes is induced by high-intensity laser power under reducing buffer conditions resulting in the reversible transition of the fluorophores into a long-lived dark state [11, 12]. Organic dyes can be coupled to a protein of interest via dye-conjugated antibodies or using self-labeling enzymes like Halo- [13], SNAP- [14], and CLIP-tags [15]. Dyes suitable for dSTORM include but are not limited to Alexa 647 and JF646 (*see* **Note 1**).

The different SMLM approaches each have their own advantages and disadvantages and the choice for the optimal technique ultimately depends on the goal of the experiment and which type of results would allow for testing the hypothesis [16–18]. This is especially true for SMLM experiments, which often involve extensive postimaging analysis [19]. For example, STORM imaging usually yields more localization events than PALM due to signal amplification by immunolabeling. Also, the organic dyes used for

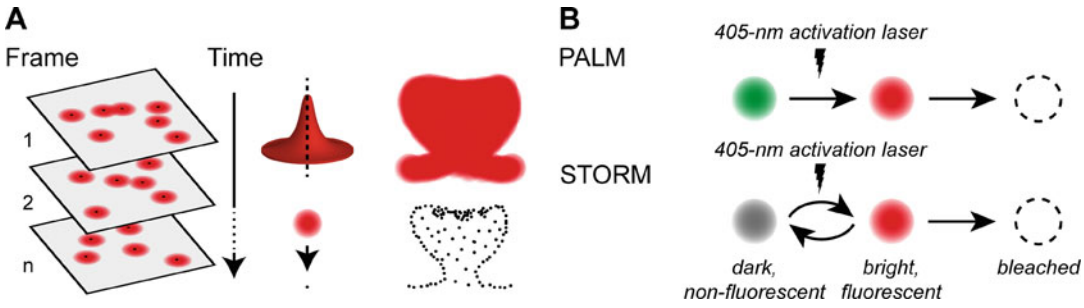

Fig. 1 Principle of single-molecule localization microscopy. (**a**) Single emitters are recorded over a large number of frames. Each identified event is fitted to localize the centroid position of the fluorophore. Together, these localizations form the reconstructed image, which is no longer diffraction limited. (**b**) PALM: fluorophores change their emission spectrum upon activation with 405 nm laser. STORM: fluorophores can reversibly switch between dark, nonemissive and bright, emissive states in a stochastic manner

STORM imaging yield a higher photon count, and thus generally result in a higher localization precision [10, 12]. On the other hand, PALM imaging is compatible with live-cell imaging, and does not require fixation and additional labeling steps, and thus effectively preserves ultrastructure.

For every fluorescence imaging technique, but particularly for SMLM, the method used to label a protein of interest is critical, as the quality of the final image depends on the properties of the fluorophore, coupling distance of the fluorophore to the protein of interest and labeling density but is also highly sensitive to experimental alterations that affect protein organization [20, 21]. Ideally, the labeling strategy should thus allow the visualization of endogenously expressed proteins using a small tag or label that yields a high signal to noise ratio, and that preserves the cellular ultrastructure (also *see* **Note 2**). We recently developed a CRISPR/Cas9-based genome editing toolbox that enables the accurate tagging of endogenous proteins in neurons, allowing the investigation of native protein complexes [22]. Importantly, this approach omits the need for specific antibodies and does not rely on overexpression of proteins that could have adverse effects.

Here we describe a SMLM protocol with three parallel workflows, each using a different labeling strategy (1) live-cell PALM using expression of mEos3.2-fused intrabodies recognizing the synaptic scaffold protein PSD-95 [23], and dSTORM making use of either (2) endogenous tagging with HaloTag [13, 22], or (3) conventional labeling using antibodies (Fig. 2a). This protocol aims to provide a starting point for setting up SMLM experiments and thus elaborates on several important experimental steps in Subheading 4. Additionally, we describe several considerations for data processing and visualization steps. As examples, the approaches are used to superresolve the distribution of endogenous synaptic receptor proteins and their scaffolds in dissociated

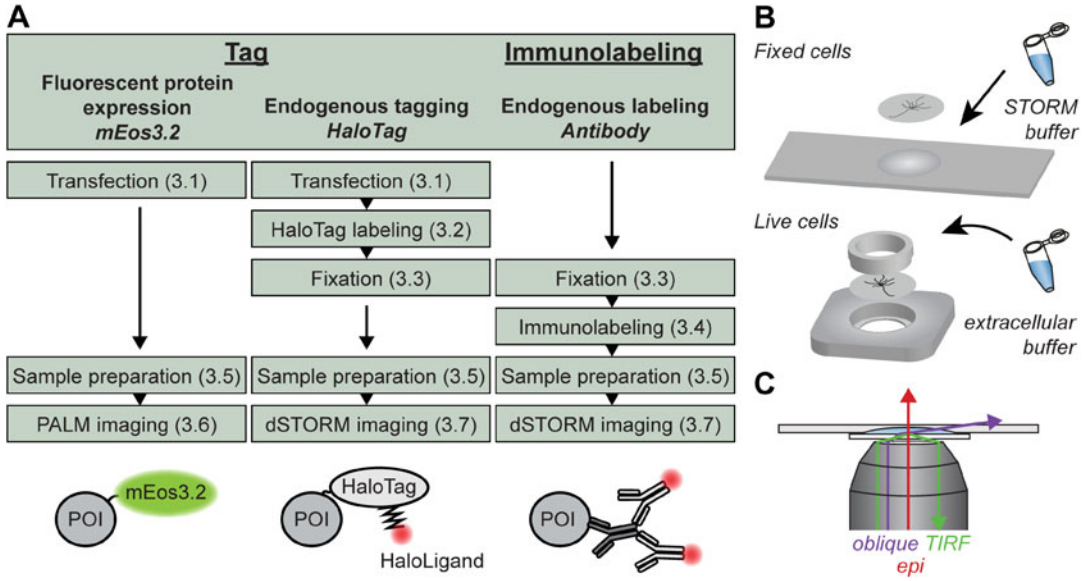

Fig. 2 SMLM experimental workflow. (**a**) Experimental workflow for 1. PALM imaging of mEos3.2, 2. dSTORM imaging of Halotag on endogenously tagged proteins, and 3. dSTORM imaging of endogenously labeled proteins. (**b**) Top: mounting of the coverslip upside down on a concave slide filled with STORM buffer. Bottom: mounting of the coverslip with live cells in a Ludin chamber with extracellular buffer on top. (**c**) Visualizing the different angles of the laser through the sample for epifluorescence, oblique illumination and TIRF imaging. POI, protein of interest

hippocampal rat neurons, but the described methodologies are, in principle, applicable to other adherent cell types.

2 Materials

2.1 Cell Culture and Transfection

1. Dissociated rat hippocampal cultures on 18-mm coverslips in 1 mL neuronal culture medium.
2. BrainPhys neuronal medium.
3. BP full medium: BrainPhys neuronal medium, 2% (v/v) NeuroCult SM1 neuronal supplement and 1% penicillin–streptomycin.
4. BP incubation medium: BrainPhys neuronal medium, 0.5 mM L-glutamine.
5. Lipofectamine 2000.
6. Water bath 37 °C.
7. Cell culture incubator (37 °C, 5% CO_2).
8. DNA plasmids: pORANGE GluA1-HaloTag knock-in [22] and PSD95.FingR-mEos3.2 [23].

2.2 HaloTag Labeling

1. HaloLigand-JF646 stock: 140 μg/mL in DMSO. Store as 1 μL single-use aliquots at −20 °C. Protect from direct light.
2. Humidified incubation chamber (plastic tray, wrapped in aluminum foil and with some moist tissues).

2.3 Fixation and Immunolabeling

1. PEM buffer: 80 mM PIPES, 2 mM MgCl2, 5 mM EGTA, pH 6.8. Filter before use (<0.3 μm filter). Store at 4 °C for a maximum of 2 weeks.
2. PFA (EM grade 32% glass ampoule). After opening, store at 4 °C in a closed tube. Warning: PFA is toxic, and quite volatile. Take proper safety precautions.
3. Fixative PEM-PFA: Dilute PFA 1:8 in PEM buffer to obtain a 4% PFA solution. Prepare fresh.
4. Phosphate buffered saline (PBS).
5. PBS-Gly: 0.1 M glycine in PBS.
6. Blocking buffer (prepare fresh): 10% (v/v) normal goat serum (NGS), 0.1% (v/v) Triton X-100 in PBS-Gly.
7. Antibody buffer (prepare fresh): 5% (v/v) normal goat serum (NGS), 0.1% (v/v) Triton X-100 in PBS-Gly.
8. Humidified incubation chamber (plastic tray, wrapped in aluminum foil and with some moist tissues).
9. Primary antibody: mouse anti-Bassoon (Enzo, RRID AB_10618753).
10. Secondary antibody: goat anti-mouse Alexa 647.

2.4 Imaging Buffers and Mounting

1. GLOX: 70 mg/mL glucose oxidase, 4 mg/mL catalase in PBS. Snap-freeze ~10 μL aliquots and store at −80 °C for up to a year. Keep thawed aliquots for maximum 1 week at 4 °C.
2. MEA stock: 1 M cysteamine in 150 mM HCl. Store as ~10 μL single-use aliquots at −80 °C for maximum 1 year. MEA is sensitive to oxygen. Prevent exposure of the powder or dissolved solution to air as much as possible.
3. Tris-glucose buffer: 50 mM Tris, 10 mM NaCl, 10% (w/v) glucose, pH 8.0. Filter through 0.2 μm filter. Store at 4 °C for up to 2 weeks, but check before use as the glucose in this buffer makes it prone to contamination.
4. STORM-buffer (prepare fresh for each coverslip, just before mounting): Add 1 μL GLOX and 0.5–2 μL MEA to 100 μL Tris-glucose buffer. Preferably, prewarm the Tris-glucose buffer.
5. Extracellular buffer: 10 mM HEPES, 120 mM NaCl, 3 mM KCl, 2 mM $CaCl_2$, 2 mM $MgCl_2$, 10 mM glucose, pH 7.35. Store at 4 °C for up to 2 weeks, but check before use as the glucose in this buffer makes it prone to contamination.

6. Concave mounting slide (for dSTORM) (Fig. 2b).
7. Vacuum pump.
8. Ludin chamber/imaging ring (for PALM) (Fig. 2b).

2.5 Microscope Setup

The imaging system described here is the setup used in our laboratory but can serve as an example to lay out the principal requirements for a suitable microscope setup. We use the commercially available Nanoimager microscope (Oxford Nanoimaging; ONI), equipped with a 100× oil-immersion objective (Olympus Plan Apo, NA 1.4) and a XYZ closed-loop piezo stage. Imaging lasers are 561 nm and 640 nm (>200 mW). Activation laser is 405 nm (>50 mW). An adjustable mirror for adjusting the angle of illumination. Camera for fluorescence detection: sCMOS (ORCA Flash 4, Hamamatsu), with an effective pixel size of 117 nm (*see* **Note 3**). Integrated filters are used to split far-red emission onto the right side of the camera and blue-green-red emission spectra on the left side. The imaging chamber can be temperature controlled. Continuous feedback control over the focus position is critical. This is built into some microscope models (as is the case for the NanoImager), or can be added with separate accessories.

2.6 Software

Integrated ONI software is used for detection and fitting of single-molecule blinking events. Alternatively, freely available options can be used: 3D-Daostorm [24], Picasso [25], Thunderstorm [26], DoM [27], ZOLA-3D [28], Fit3Dspline (integrated into SMAP) [29], SMAP [30], and Decode [31]. For additional processing steps, we use MATLAB.

3 Methods

All steps are performed at room temperature, unless mentioned otherwise. See Fig. 2a for a flowchart indicating which steps to follow for each individual method.

For direct labeling with antibodies, go to Subheading 3.3.

3.1 Transfection of Dissociated Hippocampal Rat Neurons

Perform all steps in a sterile flow hood. DNA plasmids for the generation of a Halo knock-in are transfected on day in vitro (DIV) 3, and those expressing an intrabody on DIV 14 (*see* **Note 4**).

1. Prepare fresh 300 µL BP incubation medium and 500 µL BP full medium for each coverslip to be transfected. Warm to 37 °C.
2. Prepare the lipofectamine mix by diluting 3.3 µL Lipofectamine 2000 in 100 µL BrainPhys neuronal medium (without

supplements) per coverslip to be transfected. Incubate for 5 min at room temperature.

3. For each coverslip, prepare a 1.5 mL microtube with 1 μg of DNA and add 100 μL BrainPhys neuronal medium (without supplements).
4. Add the lipofectamine mix to the DNA mix, gently mix using a pipette and incubate 30 min. DNA-Lipofectamine complex is stable for several hours at room temperature.
5. Transfer 50% (500 μL) of the conditioned medium from each well to a new 12-wells plate. Add 500 μL fresh BP full medium to each well of this new plate. Place this 'new plate' in the incubator.
6. Add 300 μL BP incubation medium to each coverslip with neurons.
7. Using a pipette, gently drop the DNA-Lipofectamine mix onto the cells and place the plate in the incubator for 1–2 h.
8. Transfer the coverslips to the 'new plate'.
9. Grow the neurons until DIV 21. Refresh half the medium with new BP full medium once a week.

For HaloTag labeling, go to Subheading 3.2. For PALM imaging, go to Subheading 3.5.

3.2 Live-Cell HaloTag Labeling

See **Note 5** for more information about self-labeling enzymes.

During the labeling procedure, prevent exposure to direct light as much as possible.

1. Prepare an incubation chamber with a piece of parafilm.
2. Dilute the HaloLigand (JF646) 1:1000 in conditioned medium (1 mL medium is enough for 12 coverslips). Mix well by pipetting up and down.
3. Place drops of ~80 μL on the parafilm and gently place the coverslips upside down on these drops. Place the incubation chamber in the incubator (37 °C, 5% CO_2) for 15 min.
4. Transfer the coverslips back to the conditioned medium and continue with fixation (Subheading 3.3) (*see* **Note 5**).

3.3 Fixation

See **Note 6** for more information about the importance of fixation and other methods.

1. Freshly prepare and prewarm PEM-PFA mixture at 37 °C.
2. Remove medium from cells using a vacuum pump and add 500 μL fixative to the coverslip. Perform this step according to the PFA MSDS and handling protocols.
3. Incubate for 5–10 min with PEM-PFA.

4. Wash 3 times 5 min with PBS-Gly (1 mL). Samples can be stored and kept stable for several days at 4 °C in PBS.

   In case of no antibody staining, go to Subheading 3.5.

3.4 Immunolabeling

1. Incubate coverslips with ~250 μL blocking buffer and incubate for 1 h at 37 °C (*see* **Note 7**).
2. Prepare primary antibody dilutions in antibody buffer (50 μL per coverslip).
3. Prepare an incubation chamber with parafilm. Place drops (~50 μL) with the antibody mixture on the parafilm and gently place the coverslips upside down on the drops.
4. Incubate for 2 h at room temperature or overnight at 4 °C (*see* **Note 7**).
5. Wash three times 5 min with PBS-Gly.
6. Dilute secondary Alexa 647-conjugated antibodies 1:400 in antibody buffer (50 μL per coverslip).
7. Incubate the coverslips as in **step 3** for 1 h (at room temperature).
8. Wash three times 5 min with PBS-Gly.
9. Postfixation (optional): Wash once with PBS (no glycine) and perform another fixation with PEM-PFA for 5 min, and wash three times with PBS-Gly (*see* **Note 8**).
10. Store the coverslips in PBS until mounting. Samples remain stable for several days if kept at 4 °C and protected from light.

3.5 Sample Preparation and Mounting

1. Preheat the microscope chamber to 37 °C.
2. Preheat extracellular buffer to 37 °C and filter (<0.3 μm filter).

3.5.1 Live-Cell PALM

3. Mount the coverslip in an imaging ring or Ludin chamber (Fig. 2b). Gently wash the coverslip once with extracellular buffer before adding up to 500 μL of extracellular buffer as final volume. Handle cells with care, try to avoid cells from drying and pipette slowly.
4. Continue at Subheading 3.6.

3.5.2 dSTORM

1. Preheat the microscope chamber to 30 °C (*see* **Note 9**).
2. Prepare fresh STORM buffer (prepare just before mounting to prevent too much exposure to air).
3. Put 100 μL STORM buffer on the concave slide and place the coverslip upside down, with the cells facing the buffer (Fig. 2b).

4. Use tweezers or a pipette tip to stabilize the coverslip. Using a vacuum pump, remove excess buffer surrounding the coverslip. Next, gently apply some pressure on top of the coverslip and remove excess buffer. Relieve the pressure slowly. Try to prevent air bubbles from entering the buffer. The coverslip should now be stably fixed to the microscope slide.
5. Continue at Subheading 3.7.

3.6 PALM Imaging

1. Locate the transfected mEos3.2-positive cell using low laser powers or light source (488-nm wavelength). Avoid long exposures, as mEos3.2 is prone to photobleaching and will be converted by 488-nm light.
2. Set acquisition parameters: The number of frames depends largely on the number of blinking events that can be detected over time. Usually, this is somewhere between 5000 and 20,000 frames. The exposure time and frame rate are of major importance for the quality of the acquisitions. For PALM imaging, we usually take a 50-ms (20 Hz) frame rate (*see* **Note 10**).
3. Set the angle of the laser to obtain oblique illumination (Fig. 2c) (*see* **Note 11**).
4. Optional: Make a snapshot of the mEos3.2 using the 488-nm laser (at low laser power). We do not recommend this for low-expressing proteins for the same reason as mentioned at **step 1** in Subheading 3.6. Alternatively, use a cotransfected marker in the far-red channel. Obtaining a diffraction-limited image can be useful for comparison with the superresolution image later on.
5. Turn on the 561-nm laser. At first, single-molecule switching events will occur without usage of the 405-nm activation laser. Suitable 561 nm laser intensity should be balanced based on the sample, with the goal being the observation of clear single-molecule events. When this is the case, start the acquisition.
6. Gradually increase 405-nm laser intensity to enhance the conversion of green to red fluorescence, but make sure the blinking events do not become too dense and start to overlap.
7. Export the acquisition as a multilayer TIF file. Continue at Subheading 3.8.

3.7 dSTORM Imaging (on Alexa 647 or HaloLigand JF646)

1. Locate cells using low laser power light source.
2. Set acquisition parameters: The number of frames depends largely on the number of blinking events that can be detected over time. Usually, this is somewhere between 5000 and 20,000 frames. The exposure time and frame rate are of major importance for the quality of the acquisitions. For

STORM, we usually take a 50-ms (20 Hz) frame rate (*see* **Note 10**).

3. Set the angle of the laser to obtain oblique illumination (Fig. 2c) (*see* **Note 11**).
4. Optional: Make a snapshot using the 640-nm laser (at low laser power). Alternatively, use a cotransfected marker in the green or red channel. Obtaining a diffraction-limited image can be useful for comparison with the superresolution image later on.
5. Turn on 640-nm laser. With high laser power, try to get most fluorophores to the dark state. Initially, and especially for samples with high labeling density, this might require slightly higher laser powers than required for imaging (*see* **Note 12**).
6. Start the acquisition as soon as blinking events can be clearly identified as individual emission events.
7. Gradually increase 405-nm laser intensity to increase the number of blinking events per frame, but make sure the blinking events do not become too dense and start to overlap.
8. When finished, export the acquisition as multilayer TIF file.

3.8 Data Processing

1. Detection and fitting of single molecules can be performed using a broad range of freely available software packages. We use ONI software integrated as part of the Nanoimager system. The software detects single emission events and uses fitting routines to estimate the coordinates of the molecules (Fig. 1a). The output is usually a results table, containing the coordinates of each fitted localization, together with parameters like the frame number, photon count and localization precision. Alternative and freely available software options are provided in Subheading 2.5.
2. Drift correction: As SMLM acquisitions take minutes to acquire, lateral drift can occur. Drift correction is a feature integrated in most processing software tools.
3. Filtering recurrent localizations (optional but strongly advised): Although many single-molecule emission events are short-lived, they can still be in the 'on state' for consecutive frames. To correct for this, these localizations can be filtered out, or merged. This feature is integrated in most processing software. If this step results in a significant reduction in the number of localizations, consider imaging with longer exposure time and higher laser power (*see* **Note 10**).
4. Filtering on localization precision: Considered one of the most important filtering steps, filtering on localization precision allows for the removal of localization events that are either the result of noise or overlapping localizations. Alternatively, or in addition to, filtering on the shape of the Gaussian can be

performed. The latter being helpful in removing overlapping emission events. We usually filter out all localizations with a localization precision of >15 nm for STORM and >25 nm for PALM imaging. This difference has to do with the fact that organic dyes provide more photons per emission event compared to fluorescent proteins, and thus a better average localization precision.

5. Filtering on photon count: Additional filtering on photon count might help to reduce the amount of noise in the dataset due to localizations derived from nonemission events. Note that localizations with a low photon count often have a low localization precision as well and most are probably filtered out when filtering just on the localization precision.

3.9 Visualization and Data Analysis

1. Rendering/Binning: The most common method of visualizing SMLM datasets is by binning the localizations into pixels. The localizations are converted to pixels and plotted as a Gaussian distribution with the standard deviation adjusted by the localization precision. Figure 3 shows examples of rendered super-resolution plots with their diffraction-limited images, for both PALM imaging of mEos3.2-tagged intrabodies targeting PSD95 and dSTORM imaging of HaloTag-GluA1 and antibody-tagged Bassoon. Commonly used pixel sizes for rendering are in the range of 10–50 nm or half the average localization precision. Combining a rendered image with a diffraction-limited snapshot of the same region, allows for visualization of the improvement in resolution and judgement of image quality as much can be learned by "just looking at the thing" [32].
2. Analyzing SMLM datasets: Extracting information about protein distribution in SMLM datasets can be challenging, and highly depends on your research question. A good way to start is exploring the heterogeneity in protein density using the molecular coordinates of the localizations instead of rendered images (Fig. 4). Density can thus not only be determined from pixel intensity but can be calculated directly from the molecular coordinates. Examples of these are the so-called local density values and Voronoi diagrams. See Fig. 4b for a comparison of these different plotting methods.
3. The local density value is calculated as the number of localizations in a given radius (in this case 5 times the mean nearest neighbor distance (MNND)) [33]. To calculate the local density, we use the MATLAB functions *knnsearch* (for determining the NND) and *rangesearch* (for the local density). The outcome can be used as color-code for plotting, as well as being used for further analysis. We use 5 times the MNND as this

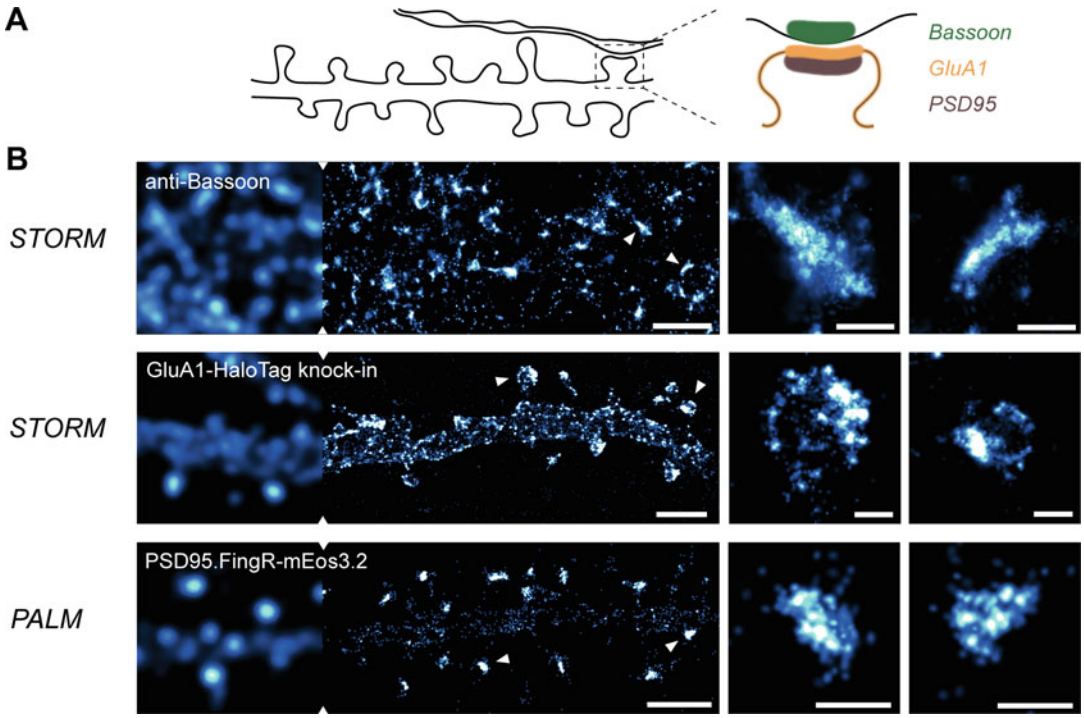

Fig. 3 SMLM of synaptic proteins. (**a**) Illustration of the expected localization of different synaptic proteins in the dendrite or axon. Scaffolding protein Bassoon localizes in the active zone of the presynaptic bouton, glutamate receptor GluA1 is localized on the dendritic membrane with an enrichment on the postsynaptic membrane, and PSD95 is a postsynaptic scaffolding protein. (**b**) Examples of dSTORM acquisitions of Bassoon using immunolabeling, endogenously tagged GluA1 with HaloTag, and live-cell PALM of PSD95 using expression of mEos3.2-fused intrabodies. Comparing the diffraction-limited image on the left part with the SMLM acquisition. Scale bars: 2 μm, zooms: 300 nm

normalizes for differences in overall localization density across the field of view and between datasets.

4. Voronoi diagrams are aimed to segment localizations into areas, reflecting the density based on the distance of each localization to its neighbors. Thus, the area of each so-called Voronoi cell reflects its density relative to the overall density of the acquisition. Voronoi diagrams can be generated using the MATLAB function *voronoi*. The area of individual Voronoi cells can be calculated from the output vertices.
5. Statistical analysis: Both the local density and Voronoi diagrams can yield important information about protein density. Further image analysis including cluster detection is often very specific to distinct biological questions. Therefore, we would like to refer to other sources for more information regarding SMLM postimaging analysis options including cluster detection, segmentation, protein counting, and colocalization [19, 34, 35].

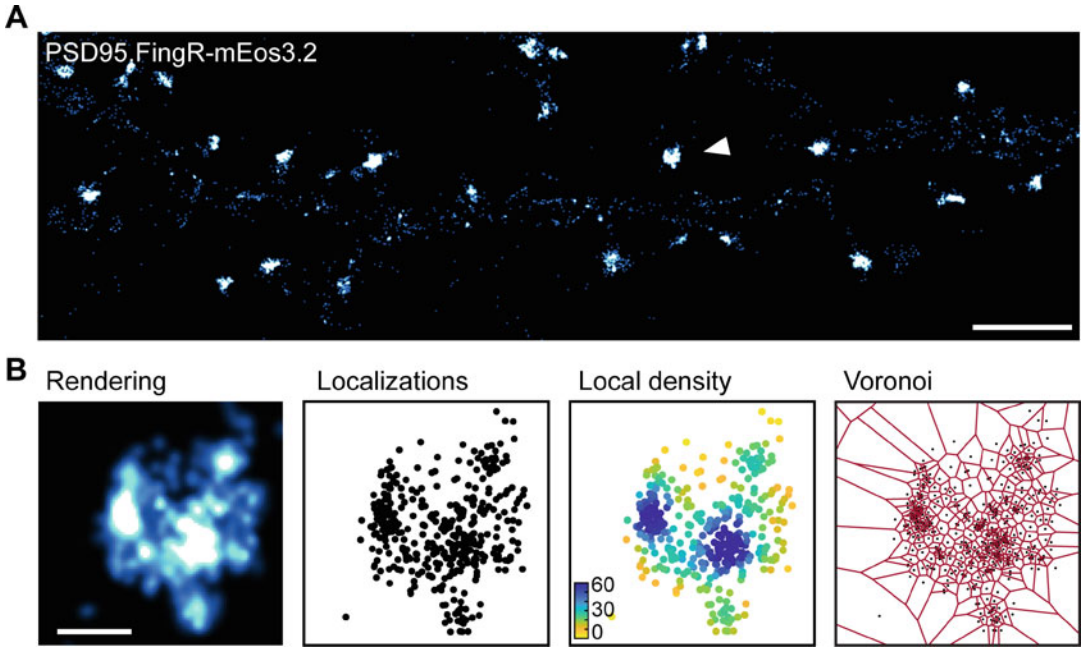

Fig. 4 Data visualization and evaluation. (**a**) Rendered image from a SMLM acquisition of PSD95.FingR-mEos3.2. (**b**) Examples of different visualization and evaluation options. Rendering: localizations are converted to pixels by plotting them as Gaussians with integrated density 1 and the localization precision as standard deviation. Localizations: Plotting the centroids of the fluorophores. Local density: Each localization is color-coded for the number of localizations within a given radius. Voronoi: Boundaries can be drawn that assign each localization to their own area that includes all points closer to that localization than any other localization. This area reflects its density relative to the overall density. Scale bar: 2 μm, zoom: 200 nm

4 Notes

1. *Dye selection for dSTORM.* Alexa 647 is considered as the best dye for dSTORM, but other dyes work as well and new dyes suitable for dSTORM are constantly being developed, mostly in the far-red emission spectrum. Besides Alexa 647 and JF646, another dye that works well in our hands is CF568. CF568 is a bit more difficult to get into the dark state (also *see* **Note 12**), and thus not advised for very dense protein structures or proteins with high expression levels. Note that imaging CF568 requires a different laser for excitation than described in the protocol (where Alexa 647 and JF646 are used).
2. *Choice of labeling method.* In our experience, protein abundance and the availability of specific antibodies are the main challenges that impact the quality of labeling, and thus the choice of method. For example, PALM on endogenous proteins is only feasible for medium to highly expressed proteins. For STORM, endogenous tagging of a protein with HaloTag can be used, but with the note that the dye to protein ratio is

much lower than labeling with antibodies. Alternatively, and not described here, proteins can be tagged with other fluorescent proteins like GFP or small epitope tags like HA, FLAG, and ALFA-tag, which can be subsequently labeled with organic dyes using antibodies or nanobodies, significantly amplifying the signal and making it possible to perform dSTORM.

3. *Pixel size*. The optimal pixel size for a given experiment depends on the number of expected photons and background. Usually, a pixel size in the range of 100–160 nm is used, based on the point spread function [2].
4. *Optimal DIV for transfection of hippocampal rat neurons*. For genomic tagging of a gene (coding for a protein of interest) we advise to transfect at a relatively young age (DIV2-5). As neurons mature, the transfection efficiency drops quite significantly. Also, and especially for proteins with a low turnover, a longer window between transfection and imaging allows for more of the protein pool to be replaced with the tagged version [22]. For exogenous expression of a fusion protein or intrabody, the optimal window between transfection and imaging day has to be optimized for individual constructs, but we usually use 3–7 days between transfection and imaging. If exogenous expression of a recombinant fusion protein is used, it is critical to make sure the level of overexpression does not alter the localization of the protein.
5. *HaloTag Ligand labeling*. HaloTag is a haloalkane dehalogenase enzyme which is designed to covalently bind to synthetic ligands (HaloLigand) [13] (Fig. 2a). The HaloTag can be coupled to the protein of interest, for example via genomic tagging (as used in this protocol), or through exogenous expression of HaloTag fusion proteins. The HaloLigand is commercially available conjugated to organic dyes. As the HaloTag—HaloLigand binding is enzymatic, live-cell labeling is preferred over labeling of already fixed samples. In addition to the protocol described here, always check the protocol of the supplier and adjust if needed. The HaloTag Ligand-JF646 used in this protocol is membrane permeable. Thus, both intracellular and extracellular HaloTag-fused proteins are labeled. The optimal length of labeling has to be determined experimentally. Extensive washing of the HaloLigand before fixation is not needed. Besides the potential harmful effects of washing on living cells, most fixatives do not react with the HaloLigand as it is not a protein. The washing steps after fixation will remove any unbound HaloLigand.
6. *Type and length of fixation*. A good fixation protocol is considered one of the most important steps of any superresolution imaging technique as it is key to the preservation of the cell's

ultrastructure. Sometimes, glutaraldehyde is used as a fixative in addition to or to replace PFA. When used, additional quenching steps (to reduce autofluorescence) using fresh $NaBH_4$ are advised. Alternatively, fixation using ice-cold methanol is sometimes used, but this is not compatible with all antibodies and might negatively influence the ultrastructure, particularly membrane-associated complexes, more than PFA. Therefore, we do not recommend this for SMLM. Although 10 min of PEM-PFA fixation is the standard, staining quality can benefit from optimizing the duration of fixation.

7. *Blocking and immunolabeling*. The protocol described here is a general protocol for immunolabeling that is used in our lab. Other blocking reagents like bovine serum albumin (BSA) can be used instead of NGS. Also, the duration and temperature of the antibody incubation step, as well as antibody concentration have to be optimized experimentally for each protein labeling.
8. *Postfixation*. Although not a must, postfixation allows for better preservation of the staining if imaging is not performed directly after labeling. Postfixed cells can be stored for several days in PBS at 4 °C.
9. *Temperature control of microscope*. Preheating and controlling the temperature of the microscope system is also advised for fixed samples. During an acquisition, heat is produced which might cause some drift, which in our hands is reduced if the temperature is already stable at around 30 °C. Therefore, we also advise to keep the STORM buffer and glass slides at least at room temperature.
10. *Exposure time, frame rate, and laser power*. Longer exposure time/lower frame rate allows for more photons to be collected from single emission events, which positively influences the localization precision. However, a long exposure time can also increase the chance of overlapping single-molecules, and when performing PALM in live cells, the movement of molecules within the exposure time of a single frame reduces the localization precision due to motion blurring. Depending on the camera, imaging smaller ROIs can allow for a higher frame rate. Alternatively, higher laser power can be used, but this reduces the lifetime of an emission event.
11. *Illumination angle*. SMLM experiments are generally performed with near TIRF illumination or so-called oblique illumination. Oblique illumination can be achieved by changing the angle of illumination toward full TIRF. Adjust the angle so that in-focus fluorescence events are mostly retained, but that out-of-focus events are not excited.
12. *Induction of dark state*. In the presence of the reducing STORM buffer, high laser power will turn molecules into the

dark state. The most common issue faced, is the inability of reducing the number of blinks per frame causing individual emission events to overlap. Using a higher concentration of MEA in the STORM buffer can help. Alternatively, 2-betamercaptoethanol (BME) is sometimes used instead of MEA, depending on the organic dye used for imaging. In our hands, using a few short pulses of the 488 nm or 561 nm laser can help to bring more far-red emitting dyes to the dark state, but with the risk of irreversible photobleaching.

Acknowledgments

This work was supported by the Netherlands Organization for Scientific Research (ALW-VIDI 171.029 to H.D.M.) and the European Research Council (ERC-StG 716011 to H.D.M.).

References

1. Vangindertael J, Camacho R, Sempels W, Mizuno H, Dedecker P, Janssen KPF (2018) An introduction to optical super-resolution microscopy for the adventurous biologist. Methods Appl Fluoresc 6(2):022003. https://doi.org/10.1088/2050-6120/aaae0c
2. Thompson RE, Larson DR, Webb WW (2002) Precise nanometer localization analysis for individual fluorescent probes. Biophys J 82(5): 2775–2783. https://doi.org/10.1016/S0006-3495(02)75618-X
3. Gould TJ, Verkhusha VV, Hess ST (2009) Imaging biological structures with fluorescence photoactivation localization microscopy. Nat Protoc 4(3):291–308. https://doi.org/10.1038/nprot.2008.246
4. Betzig E, Patterson GH, Sougrat R, Lindwasser OW, Olenych S, Bonifacino JS, Davidson MW, Lippincott-Schwartz J, Hess HF (2006) Imaging intracellular fluorescent proteins at nanometer resolution. Science 313(5793): 1642–1645. https://doi.org/10.1126/science.1127344
5. Hess ST, Girirajan TP, Mason MD (2006) Ultra-high resolution imaging by fluorescence photoactivation localization microscopy. Biophys J 91(11):4258–4272. https://doi.org/10.1529/biophysj.106.091116
6. Rust MJ, Bates M, Zhuang X (2006) Sub-diffraction-limit imaging by stochastic optical reconstruction microscopy (STORM). Nat Methods 3(10):793–795. https://doi.org/10.1038/nmeth929
7. Heilemann M, van de Linde S, Schuttpelz M, Kasper R, Seefeldt B, Mukherjee A, Tinnefeld P, Sauer M (2008) Subdiffraction-resolution fluorescence imaging with conventional fluorescent probes. Angew Chem Int Ed Engl 47(33):6172–6176. https://doi.org/10.1002/anie.200802376
8. Jungmann R, Avendano MS, Woehrstein JB, Dai M, Shih WM, Yin P (2014) Multiplexed 3D cellular super-resolution imaging with DNA-PAINT and exchange-PAINT. Nat Methods 11(3):313–318. https://doi.org/10.1038/nmeth.2835
9. Balzarotti F, Eilers Y, Gwosch KC, Gynna AH, Westphal V, Stefani FD, Elf J, Hell SW (2017) Nanometer resolution imaging and tracking of fluorescent molecules with minimal photon fluxes. Science 355(6325):606–612. https://doi.org/10.1126/science.aak9913
10. Li H, Vaughan JC (2018) Switchable fluorophores for single-molecule localization microscopy. Chem Rev 118(18):9412–9454. https://doi.org/10.1021/acs.chemrev.7b00767
11. Dempsey GT, Vaughan JC, Chen KH, Bates M, Zhuang X (2011) Evaluation of fluorophores for optimal performance in localization-based super-resolution imaging. Nat Methods 8(12):1027–1036. https://doi.org/10.1038/nmeth.1768
12. Samanta S, Gong W, Li W, Sharma A, Shim I, Zhang W, Das P, Pan W, Liu L, Yang Z, Qu J, Kim JS (2019) Organic fluorescent probes for stochastic optical reconstruction microscopy (STORM): recent highlights and future

possibilities. Coord Chem Rev 380:17–34. https://doi.org/10.1016/j.ccr.2018.08.006

13. Los GV, Encell LP, McDougall MG, Hartzell DD, Karassina N, Zimprich C, Wood MG, Learish R, Ohana RF, Urh M, Simpson D, Mendez J, Zimmerman K, Otto P, Vidugiris G, Zhu J, Darzins A, Klaubert DH, Bulleit RF, Wood KV (2008) HaloTag: a novel protein labeling technology for cell imaging and protein analysis. ACS Chem Biol 3(6): 373–382. https://doi.org/10.1021/cb800025k
14. Keppler A, Gendreizig S, Gronemeyer T, Pick H, Vogel H, Johnsson K (2003) A general method for the covalent labeling of fusion proteins with small molecules in vivo. Nat Biotechnol 21(1):86–89. https://doi.org/10.1038/nbt765
15. Gautier A, Juillerat A, Heinis C, Correa IR Jr, Kindermann M, Beaufils F, Johnsson K (2008) An engineered protein tag for multiprotein labeling in living cells. Chem Biol 15(2): 128–136. https://doi.org/10.1016/j.chembiol.2008.01.007
16. Jacquemet G, Carisey AF, Hamidi H, Henriques R, Leterrier C (2020) The cell biologist's guide to super-resolution microscopy. J Cell Sci 133(11). https://doi.org/10.1242/jcs.240713
17. Schermelleh L, Ferrand A, Huser T, Eggeling C, Sauer M, Biehlmaier O, Drummen GPC (2019) Super-resolution microscopy demystified. Nat Cell Biol 21(1):72–84. https://doi.org/10.1038/s41556-018-0251-8
18. Wait EC, Reiche MA, Chew TL (2020) Hypothesis-driven quantitative fluorescence microscopy - the importance of reverse-thinking in experimental design. J Cell Sci 133(21). https://doi.org/10.1242/jcs.250027
19. Wu YL, Tschanz A, Krupnik L, Ries J (2020) Quantitative data analysis in single-molecule localization microscopy. Trends Cell Biol 30(11):837–851. https://doi.org/10.1016/j.tcb.2020.07.005
20. Jimenez A, Friedl K, Leterrier C (2020) About samples, giving examples: optimized single molecule localization microscopy. Methods 174:100–114. https://doi.org/10.1016/j.ymeth.2019.05.008
21. Yang X, Specht CG (2020) Practical guidelines for two-color SMLM of synaptic proteins in cultured neurons. In: Yamamoto N, Okada Y (eds) Single molecule microscopy in neurobiology. Neuromethods Humana, New York, NY. https://doi.org/10.1007/978-1-0716-0532-5_9
22. Willems J, de Jong APH, Scheefhals N, Mertens E, Catsburg LAE, Poorthuis RB, de Winter F, Verhaagen J, Meye FJ, MacGillavry HD (2020) ORANGE: a CRISPR/Cas9-based genome editing toolbox for epitope tagging of endogenous proteins in neurons. PLoS Biol 18(4):e3000665. https://doi.org/10.1371/journal.pbio.3000665
23. Gross GG, Junge JA, Mora RJ, Kwon HB, Olson CA, Takahashi TT, Liman ER, Ellis-Davies GC, McGee AW, Sabatini BL, Roberts RW, Arnold DB (2013) Recombinant probes for visualizing endogenous synaptic proteins in living neurons. Neuron 78(6):971–985. https://doi.org/10.1016/j.neuron.2013.04.017
24. Babcock H, Sigal YM, Zhuang X (2012) A high-density 3D localization algorithm for stochastic optical reconstruction microscopy. Opt Nanoscopy 1(6). https://doi.org/10.1186/2192-2853-1-6
25. Schnitzbauer J, Strauss MT, Schlichthaerle T, Schueder F, Jungmann R (2017) Super-resolution microscopy with DNA-PAINT. Nat Protoc 12(6):1198–1228. https://doi.org/10.1038/nprot.2017.024
26. Ovesny M, Krizek P, Borkovec J, Svindrych Z, Hagen GM (2014) ThunderSTORM: a comprehensive ImageJ plug-in for PALM and STORM data analysis and super-resolution imaging. Bioinformatics 30(16):2389–2390. https://doi.org/10.1093/bioinformatics/btu202
27. Chazeau A, Katrukha EA, Hoogenraad CC, Kapitein LC (2016) Studying neuronal microtubule organization and microtubule-associated proteins using single molecule localization microscopy. Methods Cell Biol 131: 127–149. https://doi.org/10.1016/bs.mcb.2015.06.017
28. Aristov A, Lelandais B, Rensen E, Zimmer C (2018) ZOLA-3D allows flexible 3D localization microscopy over an adjustable axial range. Nat Commun 9(1):2409. https://doi.org/10.1038/s41467-018-04709-4
29. Li Y, Mund M, Hoess P, Deschamps J, Matti U, Nijmeijer B, Sabinina VJ, Ellenberg J, Schoen I, Ries J (2018) Real-time 3D single-molecule localization using experimental point spread functions. Nat Methods 15(5):367–369. https://doi.org/10.1038/nmeth.4661
30. Ries J (2020) SMAP: a modular super-resolution microscopy analysis platform for SMLM data. Nat Methods 17(9):870–872. https://doi.org/10.1038/s41592-020-0938-1

31. Speiser A, Muller L-R, Matti U, Obara CJ, Legant WR, Kreshuk A, Macke JH, Ries J, Turaga SC (2020) Deep learning enables fast and dense single-molecule localization with high accuracy. BioRxiv. https://doi.org/10.1101/2020.10.26.355164
32. Mund M, Ries J (2020) How good are my data? Reference standards in superresolution microscopy. Mol Biol Cell 31(19): 2093–2096. https://doi.org/10.1091/mbc.E19-04-0189
33. MacGillavry HD, Song Y, Raghavachari S, Blanpied TA (2013) Nanoscale scaffolding domains within the postsynaptic density concentrate synaptic AMPA receptors. Neuron 78(4):615–622. https://doi.org/10.1016/j.neuron.2013.03.009
34. Khater IM, Nabi IR, Hamarneh G (2020) A review of super-resolution single-molecule localization microscopy cluster analysis and quantification methods. Patterns (N Y) 1(3): 100038. https://doi.org/10.1016/j.patter.2020.100038
35. Baddeley D, Bewersdorf J (2018) Biological insight from super-resolution microscopy: what we can learn from localization-based images. Annu Rev Biochem 87:965–989. https://doi.org/10.1146/annurev-biochem-060815-014801